Journal of Engineering and Sustainable Development
https://jeasd.uomustansiriyah.edu.iq/index.php/jeasd
https://doi.org/10.31272/jeasd.27.5.8

Vol. 27, No. 05, September 2023
ISSN 2520-0917

Original Research

BIT ERROR PERFORMANCE ENHANCEMENT FOR UNDERWATER ACOUSTIC NOISE CHANNEL BY USING CHANNEL CODING

Thamer Easa Murad*, Yasin Yousif Al-Aboosi

Electrical Engineering Department, College of Engineering, Mustansiriyah University, Baghdad, Iraq
(https://orcid.org/0000-0002-9918-7770)

Received 14/11/2011 ***Accepted in revised form 21/02/2023*** ***Published 01/09/2023***

Abstract: The harm that underwater noise pollution poses to aquatic ecosystems and the resources that support it are being acknowledged on a worldwide scale. Fisheries and ecotourism are only two of the important businesses that are impacted by noise pollution. Reducing underwater impact noise is a major challenge for underwater acoustic communication systems. However, the implementation of noise reduction measures (noise abatement) remains limited. Most communication systems assume that the noise is both additive and Gaussian. Underwater Acoustic Noise (UWAN) systems generally perform poorly because of the often large non-Gaussian components in intermittent noise in the ocean. This study presents an experimental model (Dolphin-EAR DE200 Series) sound channel noise underwater at Lake Diyala Hamrin, Iraq, using a hydrophone model. Low data volume, multipath propagation, low bandwidth, and higher bit error rate (BER) of received data are major issues for underwater communication systems. In this paper, the Underwater Acoustic Channel (UWAC) aspect is evaluated and an error performance term is determined from the noise in the Student's t-distribution. In addition, Signals using binary phase-shift keying (BPSK) and quadrature phase-shift keying (QPSK) are used to generate error power analysis.

Keywords: *Channel coding; non-Gaussian distribution; polar codes; t-distribution; underwater acoustic Channel*

1. Introduction

One important technology employed in the ocean is underwater communications [1 – 3]. Most marine mammals, including dolphins and whales, "have been using acoustic waves to connect in enormous oceans for millions of years" [4]. Due to the ongoing spread of human activity in the undersea environment, there have recently been more calls for underwater communications. For instance, environmental monitoring, underwater research, academic information summarization, Maritime archaeology, oil drilling in the ocean, tactical surveillance [5 – 7], security concerns, sea investigations, etc [8].

The four types of waves electromagnetic, radio, optical, and acoustic are common information carriers for underwater communication [9,10]. Due to its distinct advantages over other contenders, the acoustic wave is the most widely used long-distance communication method [11]. Low-frequency radio waves are not ideal since they cannot travel over great distances [12]. Due to the significantly increased attenuation in the water, it is rarely used for underwater communication [13]. Although they are not as attenuated, optical waves are nevertheless in terms of energy. impacted by absorption, scattering, and high levels of ambient light, which reduces their transmission range [14, 15]. As a result, underwater communication across

*Corresponding Author: thamer1977@gmail.com

short and long distances is best accomplished using acoustic waves [12].

Three significant causes of underwater noise are background noise from the ocean, vehicle noise, and occasional noise from biological sources like rain, ice cracking, and shrimp [16]. A collection of diverse sources that are unable to be distinguished individually may also be referred to as ambient noise [17]. Acoustic communication is significantly hampered by background noise [18]. Intermittent noise, as opposed to ambient noise, frequently has significant non-Gaussian features [19].

Since the ocean's ability to dampen sound depends. The ocean can serve as a low-pass filter for background noise, depending on the operating frequency. Numerous papers demonstrate that noise, particularly in underwater communication systems, does not have a Gaussian distribution. Extremely loud noise events frequently occur. Consequently, this causes the term to be used. UWAN is distinguished by a genuine PDF with a t-distribution form and a focus on impulsive acts [16,20].

This study analyzes field experiment measurements and calculates the PDF in order to construct an experimental model for an underwater acoustic noise channel. Both the (BPSK) signal and the (QPSK) signal are used to create the formulas for the error performance analysis. Additionally, simulations using experimental noise collection were carried out to provide the error performance analysis for the UWA system.

The remainder of this essay is structured as follows. The UWAN channel's signaling model is described in Section 2. Based on data gathered on the Tigris River, Section 3 defines the outcomes of the noise model. Section 4 explains the analysis of error performance for the BPSK Signal and the QPSK Signal. Section 5 explains channel coding (convolution and polar codes). Findings and analysis are discussed in Section 6 of this article. Lastly, the conclusion to this article is detailed in Section 7

2. Signal Model

Numerous applications were built on the premise that the signal that was received in the UWAC system could be defined as [21]:

$$R[n] = T[n] + N[n] \quad (1)$$

N[n] stands for the UWAN, and T[n] represents the intended M-ary PSK or M-ary QAM signal. The assumptions about the UWAN's Gaussian distribution are detailed in [22]. A recent study, however, indicates that the UWAN may follow the student's t-distribution noise. Therefore, N[n] denotes the noise sample which belongs to the student's t-distribution. For several uses, White noise additives are primarily used with Gaussian noise. This resulted in the PDF as given [23,24]:

$$p(z) = \frac{1}{\sigma\sqrt{2\pi}} e^{-\frac{(z-\mu)^2}{2\sigma^2}} \quad (2)$$

Where μ, σ represented adjacent samples are independent of one another, all samples are Gaussian, and the mean value and standard deviation are and all samples have the same statistical features according to the auto-correlation functions' delta function. As such, it was found that the samples are considered independent and distributed identically. Since the UWAN contains many individual sources, it is necessary to accurately identify the distribution [20,24]. Numerous sources claim that the UWAN deviates from the standard distribution. Instead, because big amplitude noise occurrences occur frequently, UWAN is distinguished by having an extended tail shape that emphasizes impulsive behaviour [23,25].

3. Information Gathering in Underwater Acoustic Channel

There were several noise samples gathered. The data was gathered from the Lake Hamrin trials in Diyala, Iraq. (Longitude: 44.5829°E; Latitude: 34.07°N) on November 29, 2021. Using a hydrophone with a frequency range of audible frequencies, model: Dolphin-EAR DE200 Series, the signals were picked up at different lake depths, starting at 3 meters, 5 meters, and 7 meters. 20°C was the approximate temperature, while 4.16 m/s (8 knots) was the approximate wind speed. Fig. 1, Fig.2, and Fig.3 serve as illustrations of this

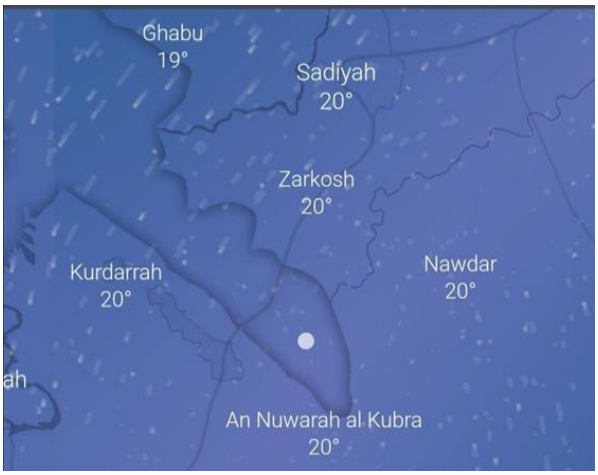

Figure 1. Place of the test in the experiment

Figure 2. Hydrophone model Dolphin EAR DE200 Series

Figure 3. Field experiments in the Lake Hamrin, Diyala, Iraq

Fig. 4 provides a waveform time visualization of the data gathered from the three heights of 3m, 5m, and 7m, where the noise's impulsive nature can be noted. For heights of 3 m, 5 m, and 7 m, Fig. 5 displays the PDF of UWAN derived from the waveform time representation. The distribution fitting tool in MATLAB can give the improved scale of t-location suitable for the sample noise PDF. A comparison of the results of the Gaussian distribution and the student t-distribution shows that the amplitude of the UWAN usually follows the student t-distribution [24]. Fig. 4 (a), (b), and (c), respectively, depict time representations of the data gathered from the three unique heights of 3 m, 5 m, and 7 m. A comparison of the normal distribution with the student's t-distribution for the PDF of the real field is shown in Fig. 5(a), (b), and (c).

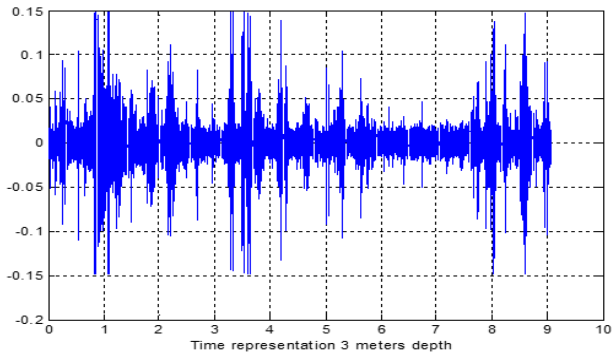

Figure 4 (a). 3 m depth

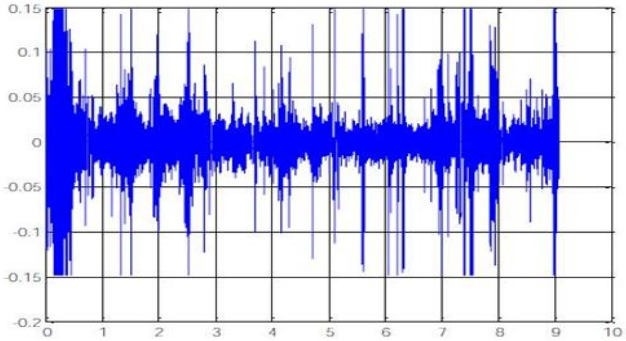

Figure 4 (b). 5 m depth

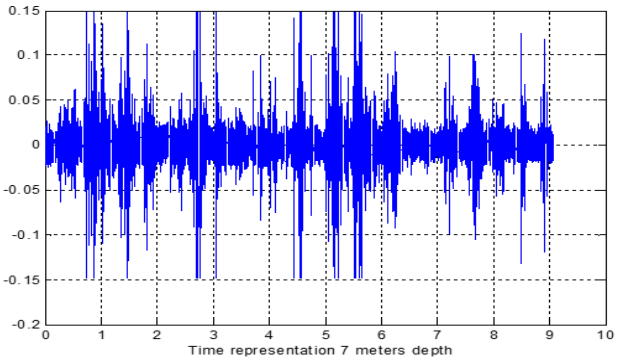

Figure 4 (c). 7 m depth

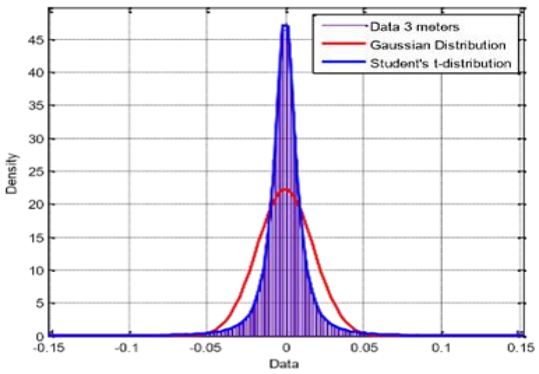

Figure 5 (a). 3 m depth

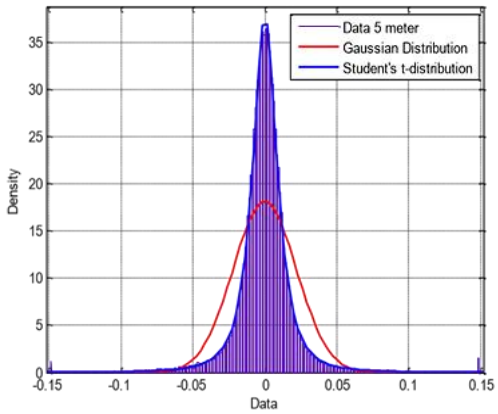

Figure 5 (b). 5 m depth

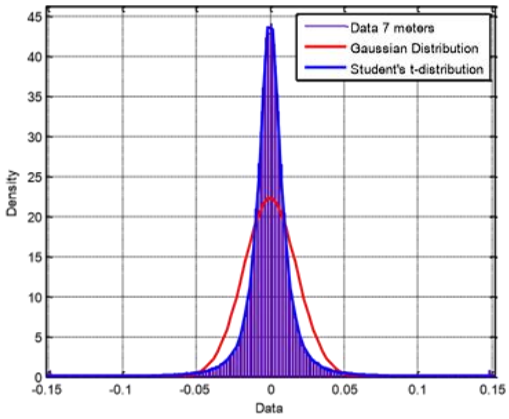

Figure 5 (c). 7 m depth

The degree of freedom at various heights of 3, 5, and 7 meters is shown in Table 1. The mean degree of freedom is 2.687. The Gaussian distribution does not match the UWAN, as shown by the low-value freedom degrees. For a brief period within the context of the overall time. According to this finding, the UWAN's state should have been stationary, Consequently, the channel with time-varying Doppler shifts and spatially variable multipath effects is ignored [19,24] and [27].

Table 1. Freedom Degrees for various depths

Various Heights (m)	Analysis Time (Sec)	Freedom Degrees (nu)
3	1.15	2.31
5	1.3	2.82
7	1.23	2.93

The t-distribution PDF is provided by [24,28]:

$$p_x(z,\ nu) = \frac{\Gamma(\frac{nu+1}{2})}{\sqrt{\pi nu}\,\Gamma(\frac{nu}{2})}\left[\frac{nu+z^2}{nu}\right]^{-(\frac{nu+1}{2})} \quad (3)$$

The gamma function is represented by Γ (·), and nu is the level of freedom that regulates the distribution's dispersion Wider PDF tails are produced by low nu values. while a high value of nu reduces the tails and converts them into a normal distribution. p_z (z, nu) represents the likelihood of finding a particular value of z and *nu* according to the t-distribution. The PDF of the t-distribution has a mean of zero (μ=0) and a variance (σ^2 = nu/ (nu -2)), for nu > 2. So, in order to simulate the volatility of a random variable (x) ($\sigma^{2)}$, the variable modifications should be carried out as follows:

$$Z=\sqrt{\frac{nu}{(nu-2)}}x \quad (4)$$

Therefore, it is possible to rewrite the probability density function for the t-distribution as follows:

$$p_x(x,\ nu) = \frac{\Gamma\left(\frac{nu+1}{2}\right)}{\sigma\sqrt{\pi(nu-2)}\,\Gamma(\frac{nu}{2})}\left[1 + \frac{x^2}{\sigma^2\,(nu-2)}\right]^{-(\frac{nu+1}{2})} \quad (5)$$

where $p_x(x,\ nu)$ is PDF in an underwater acoustic communication system, for nu = 2.687, the PDF is:

$$p_x(x,\ 2.687) = \frac{0.721}{\sigma}\left[1 + \frac{1.4556\,x^2}{\sigma^2}\right]^{-1.8435} \quad (6)$$

If roughly speaking, the average degree of freedom 3 (≅ 3) then, the PDF is:

$$p_x(x,\ 3) = \frac{0.636}{\sigma}\left[1 + \frac{x^2}{\sigma^2}\right]^{-2} \quad (7)$$

4. Underwater Acoustic Error Probability

The following sub-sections help us better understand the error probability of some modulation techniques used in this article.

4.1. BPSK Signal Error Performance Analysis

The prior PDF computation is used to evaluate the representation of the error probability for the BPSK signal in the UWAN channel, as illustrated in Fig. 6.

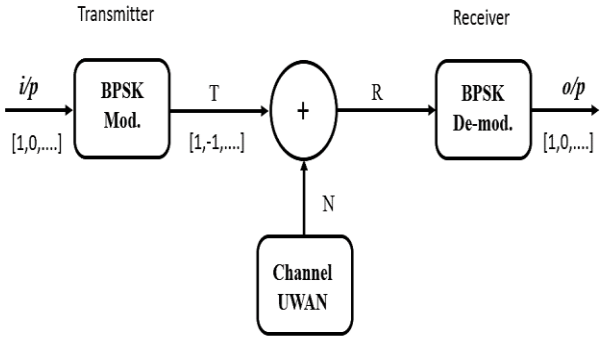

Figure 6. Block Diagram for BPSK Modulation in UWA System [23]

The error power calculation starts with the BPSK signal and the transmitted BPSK symbols, expressed as $+A = \sqrt{E_b}$ and $-A = \sqrt{E_b}$, where E_b The energy that is associated with the bit is called bit energy. nu with a value of 2.687 may be described as follows:

$$p(R/T_0) = p(x + A) = \frac{0.721}{\sigma}[1 + \frac{1.4556x^2}{\sigma^2}]^{-\,1.8435} \quad (8)$$

$$p(R/T_1) = p(x - A) = \frac{0.721}{\sigma}[1 + \frac{1.4556x^2}{\sigma^2}]^{-\,1.8435} \quad (9)$$

Thus, in detecting antipodal signals corrupted by additive noise, the error probability is binary equiprobable (BPSK) source may be determined by integrating any of the probability functions as shown below:

$$P_{BPSK} = p(T_1)p(e/T_1) + p(T_0)p\left(\frac{e}{T_0}\right) \quad (10)$$

If $p(T_1) = p(T_0) = 1/2$ then:

$$P_{BPSK} = \int_0^{\infty} p(e/T_1)\ dx \quad (11)$$

The formula for the energy per bit is Eb = A2 Tb, where Tb stands for the bit's time. The power spectral density of the average noise is less than.

The term was first coined by No = $\sigma 2\ /B$, where B = 1/2Tb represents occupied baseband bandwidth. Without sacrificing generality, presuming that the pulses' amplitudes are constant, that is to say, that the value of A is equal to one. The noise variance $\sigma 2$ is then mapped to SNR (Eb/No) as follows [21]:

$$\sigma^2 = \frac{1}{\frac{2E_b}{N_0}} \quad (12)$$

At last, by substituting. (8) and (12) in Eq. (11), the P_{BPSK} of UWAN channel for nu = 2.687 may be written as:

$$p_{BPSK} = 0.721 \sqrt{\frac{2E_b}{N_o}} \int_0^{\infty} \left[1 + \frac{2.9112}{N_o}\ (x + 1)^2\right]^{-1.8435}\ dx \quad (13)$$

Likewise, for the nu = 3, the PBPSK of UWAN channel can be written as:

$$p_{BPSK} = 0.636 \sqrt{\frac{2E_b}{N_o}} \int_0^{\infty} [+\frac{2E_b}{N_o}\ (x+1)^2]^{-2}\ dx \quad (14)$$

The theoretical BER for A channel with additive white Gaussian noise (AWGN) is provided by [29]:

$$p_{BPSK} = \frac{1}{2} erfc\ (\sqrt{\frac{E_b}{2N_o}}) \quad (15)$$

4.2. Analysis of Bit Error Performance of QPSK Signal

The QPSK constellation consists of two BPSK signals. Since noise is statistically independent of orthogonal elements, the following elements represent the two-bit sign for the likelihood of making the right choice [30]:

$$P_c = (1 - P_2)^2 \quad (16)$$

Where P_2 represents the p_{BPSK} modulation order. Given is the QPSK symbol error probability (p QPSK):

$$p_{QPSK} = 1 - P_c = 2p_{BPSK}(1 - \frac{p_{BPSK}}{2}) \quad (17)$$

When nu = 2.687, Eq. (13) is substituted into Eq. (17), so that the PQPSK of UWAN channel can be written as:

$$p_{QPSK} = 1.442 \sqrt{\frac{2E_b}{N_o}} \int_0^{\infty} \left[1 + \frac{1.4556x^2}{(13)}\right]^{-1.8435} dx\ (1 - 0.3605 \sqrt{\frac{2E_b}{N_o}} \int_0^{\infty} \left[1 + \frac{1.4556E_b}{N_o}\ (x + 1)^2\right]^{-1.8435} dx \quad (18)$$

Likewise, for the nu = 3, Eq. (14) is substituted into Eq. (17), The UWAN channel's QPSK symbol error probability is given as:

$$p_{QPSK} = 1.272 \int_0^{\infty} [1 + \frac{2E_b}{N_o}\ (x+1)^2\ ]^{-2}\ dx\ (1 - 0.318 \sqrt{\frac{2E_b}{N_o}} \int_0^{\infty} \left[1 + \frac{2E_b}{N_o}\ (x+1)^2\right]^{-2} dx \quad (19)$$

The theoretical BER of the AWGN channel for QPSK, is shown below [31]:

$$p_{QPSK} = erfc(\sqrt{\frac{E_s}{2N_o}}) - \frac{1}{4}\ erfc^2\left(\sqrt{\frac{E_s}{2N_o}}\right) \quad (20)$$

Where E_s is the energy per symbol and erfc(x) stands for the complementary error function. The likelihood of a symbol error for 16-PSK and 16-QAM modulations in the UWAN channel can also be calculated.

5. Channel Codding

Channel coding is used to correct the system's remaining flaws and approach an effective acoustic system with a noticeably stronger communication link. The primary goal is to raise the BER reduction rate to the highest possible level. Convolution and turbo codes, two-channel coding methods, have been researched in this work.

5.1 Convolution Code

Three parameters define convolutional coding (CC) (n, k, u), each of which stands for the number of memory registers, output bits, and input bits [32].

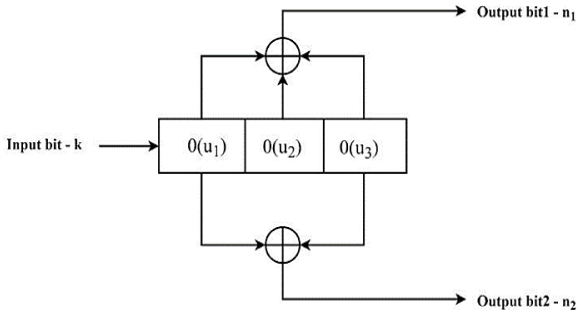

Figure 7. Convolutional encoder structure

The code rate is R = k/n, where k and n correspond to the ranges 1 to 8 and 2 to 10, respectively. can be used to calculate the code efficiency. One CC, which is defined as CC, was used (7, 5). Using the CC order and four states in a trellis form, the Viterbi algorithm is employed for decoding. Decoding can be done in two ways: hard or soft. While soft decoding takes advantage of the real values generated by the output equalisation, hard decoding just uses binary values. Alternatives for polynomials u-order codes abound. The best polynomial can be discovered through simulation and trial and error. Two generating polynomials are used in this study, determined by the bits (1 1 1) and (1 0 1), as depicted in Fig. 7 [33].

5.2 Polar Code

Polar codes are constructed using the channel polarization transformer [34]. Because some channels are very trustworthy for combining and splitting at infinite lengths while others are not, it is believed that the channels or the position of the bits would polarize in this situation. Only when data bits are deposited in trustworthy channels can the channel capacity be attained. The goal of polar code building is to identify the frozen set, which is a collection of the most unstable channels. The design-SNR component is necessary for a variety of complex construction algorithms because, although some have universal structures, polar codes do not have a uniform nature. The encoder is reflected by the kernel's polarization. Fig. 8 shows a Polar code with a length of 4 [34].

$$F = \begin{bmatrix} 1 & 0 \\ 1 & 1 \end{bmatrix}$$

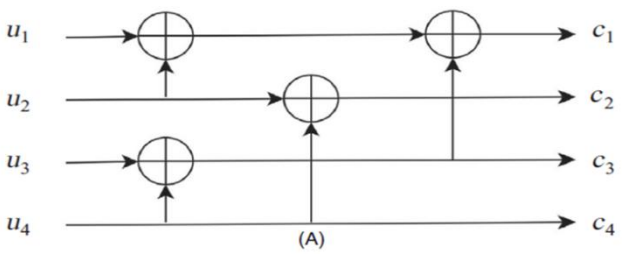

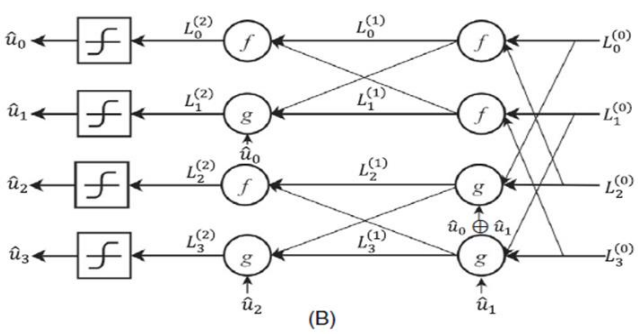

Figure.8. (A) encoder, and (B) decoder for a 4-bit polar code [34]

With this Kronecker product, a bigger input size can be obtained since it enables the polar codes using two different power lengths. Although the encoding is shown as follows, the descriptive code N refers to n=log2(N):

$$G = F^{\otimes n} \quad (22)$$

Where $\boldsymbol{F^{\otimes n}}$ stands for the n-fold increase in the Kronecker product F The encoding is represented by Fig. (8-A) for a code length of 4. (21).

$$c = uG$$

Although polar codes can be decoded via propagation, successive cancellation is the most used decoding technique (SC). From the encoder directly along the probabilistic nodes, this SC decoder can be obtained. As shown below, XOR and connection nodes are both shown. Within the LLR domain, f and g nodes conduct the following calculations for LLRs a and b [32]:

$$f(a,b) = log\left(\frac{e^{a+b}+1}{e^{a}+e^{b}}\right) \quad (23)$$

$$\mathrm{g}(a,b,s) = (-1)^{s}a + b \quad (24)$$

where the partial sum is indicated by s; The preceding decoded bits are used to create this total, which is then appended to the current g node. When $\boldsymbol{f}$ is applied to an approximation, the yield is expressed as follows:

$$f(a,b) = sign(a)sign(b)min(|a|,|b|) \quad (25)$$

The propagation of the (LLRs) in Fig. 8 (b) is from right to left (8 B). This is shown in the image as L. The first bit, u1, can be directly decoded using the proper f nodes after passing (LLRs), while u2, which requires the partial sum, needs to be decoded using the g node. When factor u1 is the only one present, the partial sum = u1. If u1 is frozen, the decoder resets the value to zero. Next, u2 is decoded using u1 and LLRs, which has a negative impact on u2 decoding performance. After making contact with every node, the decoding operation ends.

6. Findings and Analysis

For two forms of channel coding, the modulation methods (BPSK, QPSK) are examined at the UWAN channel and contrasted with the AWGN channel (convolutional and polar channel coding). Fig. 9 provides the BER as a function of *Eb/No* for (BPSK) and (QPSK) under (UWAN) channel with degrees of freedom (nu = 2.687) compared with AWGN channel. The theoretical BER of the AWGN channel computed directly from Eqs and the black line represents the simulation uncoding data result in the UWAN channel, respectively. The green with red + mark line stands for 15 and 20. The pink curve presented BER when polar channel coding was used. Where the blue curve presented BER when convolution channel coding was used.

Additionally, compared to the AWGN channel, The UWAN channel seems to have a little lower error rate. until an Eb/No level of about (4, 3.2) dB for BPSK and (7.3, 6.43) dB for QPSK respectively. Following these critical points, the probability of error as the performance gap widens to raise Eb/No values, the UWAN channel overtakes the AWGN channel in size. The PDF's shape may help to understand the behaviour on the UWAN channel at low Eb/No, despite the fact that it seems paradoxical. The

PDF of the UWAC system has wider tails and therefore a centre body that is longer than the Gaussian curve as shown in Fig. 10.

With the use of different modulation techniques, The M value for M-ary PSK and M-ary QAM modulation is increased, which lowers the bit error rate of the UWAN channel and raises the critical value for the signal-to-noise ratio (Eb/No). Additionally, it is observed when the degree of freedom (nu=2.687), The signal to noise ratio (Eb/No), and bit error rate of the UWAN channel have both improved. as shown in Table 2 for BER=10^{-5} when using polar channel coding.

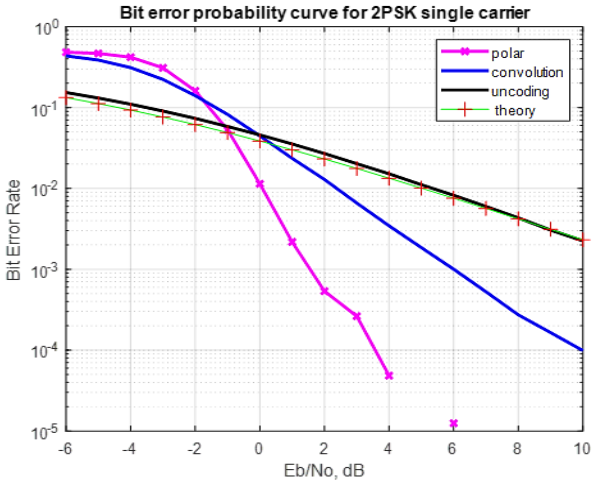

(a) BPSK at nu = 2.687

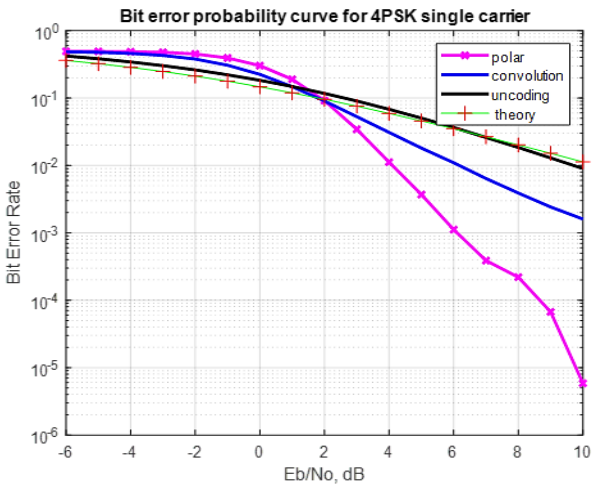

(b) QPSK at nu = 2.687

Figure 9. BPSK and QPSK symbol error performance under UWAN channel compared with AWGN channel

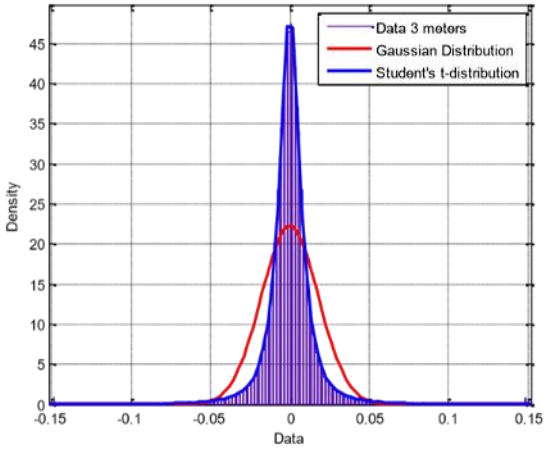

Figure 10. The function of probability density for samples of real-field noise that are three metres deep is compared using the Student's t-distribution and the Gaussian distribution.

Table 2. Eb/No Ratio for UWAN Channel at nu = 2.687 when using polar channel coding.

Type Modulation	Eb/No (dB)
BPSK	6
QPSK	9.8

As predicted, the performance when using polar code is enhanced when compared with convolutional code. For example at Eb/No =6 dB BER= 10^{-3} when using convolutional channel coding where it gives BER=10^{-5} when using polar channel coding. It is acknowledged that various error control coding techniques will be required to reduce the undesired effects of the noise, making underwater audio communication more dependable.

7. Conclusions

The Underwater acoustic noise (UWAN) demonstrates an accentuated impulsive behaviour. Therefore, to provide error enhancement for the acoustic noise channel by using suitable channel coding, polar channel coding has been proposed in this paper. With the use of different modulation techniques and different channel coding types (convolutional

and polar channel coding), the bit error rate of UWAN channel is enhanced, and the critical value for the Eb/No will be increased. Additionally, it is observed when the degree of freedom (nu=2.687), the bit error rate of UWAN channel is also improved and the Eb/No will be increased. The performance when using polar code is enhanced when compared with convolutional code as an example at Eb/No =6 dB gives BER= 10^{-3} when using convolutional channel coding where BER=10^{-5} , when using polar channel coding, The undesired effects of noise will need to be reduced using specific error control coding techniques, which will make underwater audio communication more trustworthy.

Competing interests

There is no conflict of interest, according to the authors.

Author Contribution Statement

Both authors contributed in writing and editing this manuscript. Author Yasin Yousif Al-Aboosi proposed the research problem and supervised the findings of this work. Authors Thamer Easa Murad, developed the introduction and the manuscript pattern. All authors discussed the results and contributed to the final manuscript.

Abbreviations:

B	occupied bandwidth
E_b	bit energy
E_s	energy per symbol
erfc(x)	complementary error function
N[n]	UWAN
nu	degree of freedom
P_2	modulation order
$p_x(x, nu)$	underwater acoustic communication system
s	partial sum
T_b	bit duration
T[n]	M-ary signal
μ	mean value
σ	standard deviation
Γ (·)	gamma function

References

1. A. Z. Sha'ameri, Y. Y. Al-Aboosi, and N. H. H. Khamis, 2019, "Underwater acoustic noise characteristics of shallow. https://doi.org/10.1109/ICCCE.2014.34
2. Attenuation and Propagation Loss for Aqueous Solution of Sodium Chloride," in 2019 International Conference on Recent Advances in Energy-efficient Computing and Communication (ICRAECC), pp. 1–5. https://doi.org/10.1109/ICRAECC43874.2019.8995039
3. Y. Y. Al-Aboosi, A. Z. Bin Sha'ameri, and N. H. H. Khamis, 2016, "Comparison of methodologies for signal detection in underwater acoustic noise in shallow tropical waters," ARPN J Eng Appl Sci, vol. 11, no. 5, pp. 3086–3094.
4. D. H. Cato, 2008, "Ocean ambient noise: its measurement and its significance to marine animals," Proc. Inst. Acoust., vol. 30, no. 5, pp. 1–9.
5. F. Hanson and S. Radic, 2008, "High bandwidth underwater optical communication," Appl. Opt., vol. 47, no. 2, pp. 277– 283. https://doi.org/10.1364/AO.47.000277
6. G. Burrowes and J. Y. Khan, 2011, "Short-range underwater acoustic communication networks," Auton. Underw. Veh., pp. 173–198. https://doi.org/10.5772/24098
7. H. Kaushal and G. Kaddoum, 2016, "Underwater optical wireless communication," IEEE Access, vol. 4, pp.

1518–1547. https://doi.org/10.1109/ACCESS.2016.2552538

8. J. G. Proakis and M. Salehi, 2008, Digital communications. McGraw-Hill.
9. J. Li, 2017, "Advanced OFDM Receivers for Underwater Acoustic Communications." University of York.
10. J. R. Barry, E. A. Lee, and D. G. Messerschmitt, 2012, Digital communication. Springer Science & Business Media.
11. J. S. G. Panaro, F. R. B. Lopes, L. J. Matos, L. M. Barreira, and I. I. N. O. M. Odel, "Empirical Noise Model.
12. J. S. G. Panaro, F. R. B. Lopes, L. M. Barreira, and F. E. Souza, 2012, "Underwater acoustic noise model for shallow water communications. https://doi.org/10.14209/SBRT.2012.85
13. J. Zhang, L. Kou, Y. Yang, F. He, and Z. Duan, 2020, "Monte-Carlo-based optical wireless underwater channel modelling with oceanic turbulence," Opt. Commun., vol. 475, p. 126214. https://doi.org/10.1016/j.apsb.2018.10.005
14. K. Chen, M. Ma, E. Cheng, F. Yuan, and W. Su, 2014, "A survey on MAC protocols for underwater wireless sensor networks," IEEE Commun. Surv. Tutorials, vol. 16, no. 3, pp. 1433–1447. https://doi.org/10.1053/j.ajkd.2016.01.020
15. L. Lanbo, Z. Shengli, and C. Jun Hong, 2008, "Prospects and problems of wireless communication for underwater sensor networks," Wirel. Commun. Mob. Comput., vol. 8, no. 8, pp. 977–994.
16. L. Liao, 2018, "Underwater Acoustic Localization with Applications to Multiuser Communications." University of York.
17. Likelihood Metrics for Underwater Acoustic Communications," 2012, Proc. IEEE Conf. Underw. Commun. Netw., no. 2, pp. 1–8. https://doi.org/10.1109/OCEANS.1993.326226
18. M. Ahsanullah, B. M. G. Kibria, and M. Shakil, 2014, "Normal distribution," in Normal and Student´ st Distributions and Their Applications, Springer, pp. 7–50. https://doi.org/10.2991/978-94-6239-061-4
19. M. C. Domingo, "Magnetic induction for underwater wireless communication networks," IEEE Trans. Antennas Propag., vol. 6, no. 60, pp. 2929–2939, 2012. https://doi.org/10.1109/TAP.2012.2194670
20. M. S. Ahmed et al., 2020, "Filter orthogonal frequency division multiplexing scheme based on polar code in underwater acoustic communication with non-gaussian distribution noise," ETRI J. https://doi.org/10.4218/etrij.2019-0564
21. M. S. Ahmed, N. S. M. Shah, F. Ghawbar, Y. A. Jawhar, and A. A. Almohammedi, 2020,"Filtered-OFDM with channel coding based on T-distribution noise for underwater acoustic communication," J. Ambient Intell. Humaniz. Comput., pp. 1–14. https://doi.org/10.1007/s12652-020-01713-9
22. M. Stojanovic and J. Preisig, 2009, "Underwater acoustic communication channels: Propagation models and statistical characterization," IEEE Commun. Mag., vol. 47, no. 1, pp. 84–89. https://doi.org/10.1109/MCOM.2009.4752682
23. N.-S. N. Ismail, L. A. Hussein, and S. H. S. Ariffin, 2010, "Analyzing the performance of acoustic channel in

underwater wireless sensor network (UWSN)," in 2010 Fourth Asia International Conference on Mathematical/Analytical Modelling and Computer Simulation, pp. 550–555. https://doi.org/10.1109/AMS.2010.111

24. R. Headrick and L. Freitag, 2009, "Growth of underwater communication technology in the US Navy," IEEE Commun. Mag., vol. 47, no. 1, pp. 80–82. https://doi.org/10.1109/MCOM.2009.4752681
25. R. P. Hodges.Underwater acoustics: 2011, Analysis, design and performance of sonar: John Wiley & Sons.
26. S. Al-Dharrab, M. Uysal, and T. M. Duman, 2013, "Cooperative underwater acoustic communications [accepted from open call]," IEEE Commun. Mag., vol. 51, no. 7, pp. 146–153. 1 https://doi.org/10.1109/MCOM.2013.6553691
27. S. Banerjee and M. Agrawal, 2014, "On the performance of underwater communication system in noise with Gaussian mixture statistics," in 2014 Twentieth National Conference on Communications (NCC), pp. 1–6. https://doi.org/10.1109/NCC.2014.6811369
28. Z. Zeng, S. Fu, H. Zhang, Y. Dong, and J. Cheng, 2016: "A survey of underwater optical wireless communications," IEEE Commun. Surv. tutorials, vol. 19, no. 1, pp. 204–238. https://doi.org/10.1109/COMST.2016.2618841
29. S. Jiang, 2019, Wireless networking principles: from terrestrial to underwater acoustic. Springer,
30. T. Melodia et al., 2013, "Advances in Underwater Acoustic Networking." Wiley Online Library. https://doi.org/10.1002/9781118511305.ch23
31. W. Sun, 2014 "Online Learning of the Spatial-Temporal Channel Variation in Underwater Acoustic Communication Networks." Michigan Technological University. https://doi.org/10.37099/mtu.dc.etdr/934
32. Tahir, B., Schwarz, S., & Rupp, M. (2017). BER comparison between Convolutional, Turbo, LDPC, and Polar codes. 2017 24th International Conference on Telecommunications (ICT), 1-7. https://doi.org/10.1109/ICT.2017.7998249
33. Bernard S (2001)." Digital communications fundamentals and applications". Prentice Hall, Upper Saddle River.
34. E. Arikan, Channel polarization: A method for constructing capacity-achieving codes for symmetric binary-input memoryless channels, IEEE Trans. Inf. Theory 55 (2009), 3051–3073.